

**Title:** How do biological traits affect brachiopod taxonomic  
2 survival? A hierarchical Bayesian approach.

**Running title:** How do biological traits affect taxonomic survival?

4 **Author:** Peter D Smits, psmits@uchicago.edu, Committee on Evolutionary  
Biology, University of Chicago

6 **Keywords:** extinction, macroevolution, macroecology, Paleozoic, selection

**Word count:** ?

8 **Table count:** 0

**Figure count:** 9

10 **Data archival location:** Dryad?

## Abstract

12 While the effect of geographic range on extinction risk is well  
documented, the effects of other traits are less well known. Here, I analyze  
14 patterns of Paleozoic brachiopod genus durations and their relationship to  
geographic range, affinity for epicontinental seas versus open ocean  
16 environments, and body size. Additionally, I allow for environmental  
affinity to have a nonlinear effect on duration. Using a hierarchical  
18 Bayesian modeling approach, I also model the possible interaction between  
the effects of the biological traits and a taxon’s time of origination. I find  
20 evidence that as extinction risk increases, the expected strength of the  
selection gradient on biological traits (except body size) increases. This  
22 manifests as greater expected differences in extinction risk for each unit  
change in geographic range and environmental preference during periods  
24 of high extinction risk, as opposed to a much flatter expected selection  
gradient during periods of low extinction risk. I find weak evidence for a  
26 nonlinear relationship between environmental preference and extinction  
risk such that “generalists” have a lower expected extinction risk than  
28 either “specialists”. Interestingly, I find that as extinction risk increases,  
the peakedness of this relationship is expected to increase as well. These  
30 results demonstrate the importance of directly modeling the structure  
inherent in the observed data as a means to better understand which  
32 processes may have been driving the observed patterns of diversification.

## 1 Introduction

34 How do biological traits affect extinction risk? Jablonski (1986) observed that  
during periods of high expected extinction risk, the effects of biological traits on  
36 survival decreased in importance. However, this pattern was weakest/absent in  
the effect of geographic range on survival (Jablonski, 1986). Biological traits are

38 defined here as descriptors of a taxon’s adaptive zone, which is the set of  
biotic–biotic and biotic–abiotic interactions that a taxon can experience. In  
40 effect, these are descriptors of a taxon’s broad-sense ecology.

Jablonski (1986) phrased their conclusions in terms of background versus mass  
42 extinction, but this scenario is readily transferable to a continuous variation  
framework as there is no obvious distinction in terms of extinction rate between  
44 these two states (Wang, 2003). I adopt a continuous variation framework as this  
is more amenable for modeling the relationship between taxon traits and  
46 extinction risk. Additionally, the Jablonski (1986) scenario has strong model  
structure requirements in order to test its proposed macroevolutionary  
48 mechanism. Not only do the taxon trait effects need to be modeled, but the  
relationships between these effects need to be modeled as well.

50 Two possible macroevolutionary mechanisms which may underly the pattern  
observed by Jablonski (1986) are: the effect of geographic range on predictive  
52 survival remains constant and those of other biological traits decrease, and the  
effect of geographic range in predicting survival increases and those of other  
54 biological traits stay constant.

I model taxon durations because trait based differences in extinction risk should  
56 manifest as differences in taxon durations. Namely, a species with a beneficial  
trait should survive longer, on average, than a species without that beneficial  
58 trait. Conceptually, taxon survival can be considered an aspect of “taxon fitness”  
along with expected lineage branching/origination rate (Cooper, 1984, Palmer  
60 and Feldman, 2012). The analysis of taxon durations, or time from origination  
to extinction, falls under the purview of survival analysis, a field of applied  
62 statistics commonly used in health care (Klein and Moeschberger, 2003) but has  
a long history in paleontology (Simpson, 1944, 1953, Van Valen, 1973, 1979).

64 Geographic range is widely considered the most important taxon trait for  
 estimating differences in extinction risk at nearly all times with large geographic  
 66 range associated with low extinction risk (Jablonski, 1986, 1987, Jablonski and  
 Roy, 2003, Payne and Finnegan, 2007). I expect this to hold true nearly always.  
 68 Miller and Foote (2009) demonstrated that during several mass extinctions taxa  
 associated with open ocean environments tend to have a greater extinction risk  
 70 than those taxa associated with epicontinental seas. During periods of  
 background extinction, however, they found no consistent difference between  
 72 taxa favoring either environment. Because of this study, the following prediction  
 for survival patterns can be made: as extinction risk increases, taxa associated  
 74 with open ocean environments should generally increase in extinction risk versus  
 those that favor epicontinental seas.  
 76 There is also a possible nonlinear relationship between environmental preference  
 and taxon duration. A long standing hypothesis is that generalists or  
 78 unspecialized taxa will have greater survival than specialists (Baumiller, 1993,  
 Liow, 2004, 2007, Nürnberg and Aberhan, 2013, 2015, Simpson, 1944) SMITS,  
 80 IN PREP. I allowed for environmental preference to possibly have a parabolic  
 effect on species duration  
 82 Body size, measured as shell length (Payne et al., 2014), was also considered as  
 a potentially informative covariate. Body size is a proxy for metabolic activity  
 84 and other, correlated, life history traits (Payne et al., 2014). There is no strong  
 hypothesis of how body size effects extinction risk in brachiopods, meaning a  
 86 positive, negative, or null effect are all plausible.  
 I adopt a hierarchical Bayesian survival modeling approach, which represents a  
 88 conceptual and statistical unification of the paleontological dynamic and cohort  
 survival analytic approaches (Baumiller, 1993, Foote, 1988, Raup, 1975, 1978,

90 Simpson, 2006, Van Valen, 1973, 1979). By using a Bayesian framework I am  
able to quantify the uncertainty inherent in the estimates of the effects of  
92 biological traits on survival, especially in cases where the covariates of interest  
(biological traits) are themselves known with error.

## 94 2 Materials and Methods

### 2.1 Analytical approach

96 Hierarchical modelling, sometimes called “mixed-effects modeling,” is a  
statistical approach which explicitly takes into account the structure of the  
98 observed data in order to model both the within and between group variance  
(Gelman et al., 2013, Gelman and Hill, 2007). The units of study (e.g. genera)  
100 each belong to a single grouping (e.g. origination cohort). These groups are  
considered draws from a shared probability distribution (e.g. all cohorts,  
102 observed and unobserved). The group-level parameters are then estimated  
simultaneously as the other parameters of interest (e.g. covariate effects)  
104 (Gelman et al., 2013). The subsequent estimates are partially pooled together,  
where parameters from groups with large samples or effects remain large while  
106 those of groups with small samples or effects are pulled towards the overall  
group mean.

108 This partial pooling is one of the greatest advantages of hierarchical modeling.  
By letting the groups “support” each other, parameter estimates then better  
110 reflect our statistical uncertainty. Additionally, this partial pooling helps control  
for multiple comparisons and possibly spurious results as effects with little  
112 support are drawn towards the overall group mean (Gelman et al., 2013,  
Gelman and Hill, 2007).

114 All covariate effects (regression coefficients), as well as the intercept term  
 (baseline extinction risk), were allowed to vary by group (origination cohort).  
 116 The covariance/correlation between covariate effects was also modeled. This  
 hierarchical structure allows inference for how covariates effects may change  
 118 with respect to each other while simultaneously estimating the effects  
 themselves, propagating our uncertainty through all estimates.

120 Additionally, instead of relying on point estimates of environmental affinity, I  
 treat environmental affinity as a continuous measure of the difference between  
 122 the taxon’s environmental occurrence pattern and the background occurrence  
 pattern (Appendix A).

## 124 **2.2 Fossil occurrence information**

The dataset analyzed here is derived from the a combination of the occurrence  
 126 information from Foote and Miller (2013) and the body size data from Payne  
 et al. (2014). The Foote and Miller (2013) dataset is based on the Paleobiology  
 128 Database (<http://www.paleodb.org>); see Foote and Miller (2013) for a full  
 description of the inclusion criterion. Additionally, epicontinental versus open  
 130 ocean assignemnts for occurrence information are based on Miller and Foote  
 (2009). NOTE: I DON’T KNOW HOW THIS MAY NEED TO BE UPDATED.

132 Sampled occurrences were restricted to those with paleolatitude and  
 paleolongitude coordinates, assignment to either epicontinental or open-ocean  
 134 environment, and belonging to a genus present in the body size dataset (Payne  
 et al., 2014). Genus duration was calculated as the number of geologic stages  
 136 from first appearance to last appearance, inclusive. Genera with a last  
 occurrence in or after Changhsingian stage were right censored at the  
 138 Changhsingian. Genera with a duration of only one stage were left censored

(Appendix C). The covariates used to model genus duration were geographic  
140 range size ( $r$ ), environmental preference ( $v, v^2$ ), and body size ( $m$ ).

Geographic range was calculated using an occupancy approach. First, all  
142 occurrences were projected onto an equal-area cylindrical map projection. Each  
occurrence was then assigned to one of the cells from a  $70 \times 34$  regular raster  
144 grid placed on the map. Each grid cell represents approximately 250,000 km<sup>2</sup>.  
The map projection and regular lattice were made using shape files from  
146 <http://www.natureearthdata.com/> and the **raster** package for R (Hijmans,  
2015).

For each stage, the total number of occupied grid cells, or cells in which a fossil  
148 occurs, was calculated. Then, for each genus, the number of grid cells occupied  
by that genus was calculated. Dividing the genus occupancy by the total  
150 occupancy gives the relative occupancy of that genus. Mean relative genus  
occupancy was then calculated as the mean of the per stage relative occupancies  
152 of that genus.

Body size data was sourced directly from Payne et al. (2014). Because those  
154 measurements are presented without error, a measurement error model similar  
to the one for environmental affinity could not be implemented (Appendix A).  
156

Prior to analysis, geographic range and body size were transformed and  
158 standardized in order to improve interpretability of the results. Geographic  
range, which can only vary between 0 and 1, was logit transformed. Body size,  
160 which is defined for all positive real values, was natural log transformed. These  
covariates were then standardized by mean centering and dividing by two times  
162 their standard deviation following Gelman and Hill (2007).

## 2.3 Survival model

164 Genus durations were modeled as time-till-event data (Klein and Moeschberger, 2003), with covariate information used in estimates of extinction risk as a  
166 hierarchical regression model. Genus durations were assumed to follow either an exponential or Weibull distribution. Each of these distributions makes  
168 assumptions about how duration may effect extinction risk (Klein and Moeschberger, 2003). The exponential distribution assumes that extinction risk  
170 is independent of duration. In contrast, the Weibull distribution allows for age dependent extinction via the shape parameter  $\alpha$ , though only as a monotonic  
172 function of duration. Importantly, the Weibull distribution is equivalent to the exponential distribution when  $\alpha = 1$ .

174 The following variables are defined:  $y_i$  is the duration of genus  $i$  in geologic stages,  $X$  is the matrix of covariates including a constant term,  $B_j$  is the vector  
176 of regression coefficients for origination cohort  $j$ ,  $\Sigma$  is the covariance matrix of the regression coefficients,  $\tau$  is the vector of scales the standard deviations of  
178 the between-cohort variation in regression coefficient estimates, and  $\Omega$  is the correlation matrix of the regression coefficients.



180 The exponential model is defined

$$\begin{aligned}
y_i &\sim \text{Exponential}(\lambda) \\
\lambda_i &= \exp(\mathbf{X}_i B_{j[i]}) \\
B &\sim \text{MVN}(\vec{\mu}, \Sigma) \\
\Sigma &= \text{Diag}(\vec{\tau}) \Omega \text{Diag}(\vec{\tau}) \\
\mu_\kappa &\sim \begin{cases} \mathcal{N}(0, 5) & \text{if } k \neq r, \text{ or} \\ \mathcal{N}(-1, 1) & \text{if } k = r \end{cases} \\
\tau_\kappa &\sim \text{C}^+(1) \text{ for } \kappa \in 1 : k \\
\Omega &\sim \text{LKJ}(2).
\end{aligned} \tag{1}$$

Similarly, the Weibull model is defined

$$\begin{aligned}
y_i &\sim \text{Weibull}(\alpha, \sigma) \\
\sigma_i &= \exp\left(\frac{-(\mathbf{X}_i B_{j[i]})}{\alpha}\right) \\
B &\sim \text{MVN}(\vec{\mu}, \Sigma) \\
\Sigma &= \text{Diag}(\vec{\tau}) \Omega \text{Diag}(\vec{\tau}) \\
\alpha &\sim \text{C}^+(2) \\
\mu_k &\sim \begin{cases} \mathcal{N}(0, 5) & \text{if } k \neq r, \text{ or} \\ \mathcal{N}(-1, 1) & \text{if } k = r \end{cases} \\
\tau_k &\sim \text{C}^+(1) \\
\Omega &\sim \text{LKJ}(2).
\end{aligned} \tag{2}$$

182 The principle difference between this model and the previous (Eq. 1) is the inclusion of the shape parameter  $\alpha$ . Note that  $\sigma$  is approximately equivalent to

184  $1/\lambda$ .

For an explanation of how this model was developed and parameter  
186 explanations, please see Appendix B. Note that these models (Eq. 1, 2) do not  
include how the uncertainty in environmental affinity is included nor how  
188 censored observations are included. For an explanation of both of these aspects,  
see Appendices A and C.

## 190 **2.4 Parameter estimation**

The joint posterior was approximated using a Markov-chain Monte Carlo  
192 routine that is a variant of Hamiltonian Monte Carlo called the No-U-Turn  
Sampler (Hoffman and Gelman, 2014) as implemented in the probabilistic  
194 programming language Stan (Stan Development Team, 2014a). The posterior  
distribution was approximated from four parallel chains run for 10,000 draws  
196 each, split half warm-up and half sampling and thinned to every 10th sample for  
a total of 5000 posterior samples. Chain convergence was assessed via the scale  
198 reduction factor  $\hat{R}$  where values close to 1 ( $\hat{R} < 1.1$ ) indicate approximate  
convergence. Convergence means that the chains are approximately stationary  
200 and the samples are well mixed (Gelman et al., 2013).

## **2.5 Model evaluation**

202 Models were evaluated using both posterior predictive checks and an estimate of  
out-of-sample predictive accuracy. The motivation behind posterior predictive  
204 checks as tools for determining model adequacy is that replicated data sets  
using the fitted model should be similar to the original data (Gelman et al.,  
206 2013). Systematic differences between the simulations and observations indicate

weaknesses of the model fit. An example of a technique that is very similar  
208 would be inspecting the residuals from a linear regression.

The strategy behind posterior predictive checks is to draw simulated values  
210 from the joint posterior predictive distribution,  $p(y^{rep}|y)$ , and then compare  
those draws to the empirically observed values (Gelman et al., 2013). To  
212 accomplish this, for each replicate, a single value is drawn from the marginal  
posterior distributions of each regression coefficient from the final model as well  
214 as  $\alpha$  for the Weibull model (Eq. 1, 2). Then, given the covariate information  $\mathbf{X}$ ,  
a new set of  $n$  genus durations are generated giving a single replicated data set  
216  $y^{rep}$ . This is repeated 1000 times in order to provide a distribution of possible  
values that could have been observed given the model.

218 In order to compare the fitted model to the observed data, various graphical  
comparisons or test quantities need to be defined. The principal comparison  
220 used here is a comparison between non-parameteric approximation of the  
survival function  $S(t)$  as estimated from both the observed data and each of the  
222 replicated data sets. The purpose of this comparison is to determine if the  
model approximates the same survival/extinction pattern as the original data.

224 The exponential and Weibull models were compared for out-of-sample predictive  
accuracy using the widely-applicable information criterion (WAIC) (Watanabe,  
226 2010). Out-of-sample predictive accuracy is a measure of the expected fit of the  
model to new data. However, because the Weibull model reduces to the  
228 exponential model when  $\alpha = 1$  my interest is not in choosing between these  
models. Instead, comparisons of WAIC values are useful for better  
230 understanding the effect of model complexity on out-of-sample predictive  
accuracy. The calculation of WAIC used here corresponds to the “WAIC 2”  
232 formulation recommended by Gelman et al. (2013). For an explanation of how  
WAIC is calculated, see Appendix D. Lower values of WAIC indicate greater

234 expected out-of-sample predictive accuracy than higher values.

### 3 Results

236 As stated above, posterior approximations for both the exponential and Weibull  
models achieved approximate stationarity after 10,000 steps, as all parameter  
238 estimates have an  $\hat{R} < 1.1$ .

Comparisons of the survival functions estimated from 1000 posterior predictive  
240 data sets to the estimated survival function of the observed genera demonstrates  
that both the exponential and Weibull models approximately capture the  
242 observed pattern of extinction (Fig. 1). The major difference in fit between the  
two models is that the Weibull model has a slightly better fit for longer lived  
244 taxa than the exponential model.

Additionally, the Weibull model is expected to have slightly better out-of-sample  
246 predictive accuracy when compared to the exponential model (WAIC 4577  
versus 4605, respectively). 1). Because the difference in WAIC between these  
248 two models is large, while results from both the exponential and Weibull models  
will be presented, only those from the Weibull model will be discussed.

250 Estimates of the overall mean covariate effects  $\mu$  can be considered  
time-invariant generalizations for brachiopod survival during the Paleozoic  
252 SMITS IN PREP (Fig. 2). Consistent with prior expectations, geographic range  
size has a negative effect on extinction risk, where genera with large ranges  
254 having greater durations than genera with small ranges.

I find that there is an approximately 93% posterior probability that the overall  
256 effect of increasing body size decreases expected extinction risk. This parameter,  
however, is not very large and is within two standard deviations of 0 (mean

258  $\mu_m = -0.15$ , standard deviation 0.1). Because of this, I interpret this as weak  
evidence for increases in body size to be associated with a decrease in expected  
260 extinction risk.

Interpretation of the effect of environmental preference  $v$  on duration is slightly  
262 more involved. Because a quadratic term is the equivalent of an interaction  
term, both  $\mu_v$  and  $\mu_{v^2}$  have to be interpreted together because it is illogical to  
264 change values of  $v$  without also changing values  $v^2$ . To determine the nature of  
the effect of  $v$  on duration I calculated the multiplicative effect of environmental  
266 preference on extinction risk.

Given mean estimated extinction risk  $\tilde{\sigma}$ , we can define the extinction risk  
268 multiplier of an observation with environmental preference  $v_i$  as

$$\frac{\tilde{\sigma}_i}{\tilde{\sigma}} = f(v_i) = \exp\left(\frac{-(\mu_v v_i + \mu_{v^2} v_i^2)}{\alpha}\right). \quad (3)$$

This function  $f(v_i)$  has a y-intercept of  $\exp(0)$  or 1 because it does not have a  
270 non-zero intercept term. Equation 3 can be either concave up or down. A  
concave down  $f(v_i)$  may indicate that genera of intermediate environmental  
272 preference have greater durations than either extreme, and *vice versa* for  
concave up function.

274 The expected effect of environmental preference as a multiplier of expected  
extinction risk can then be visualized (Fig. 3). This figure depicts 1000 posterior  
276 predictive estimates of Eq. 3 across all possible values of  $v$ . The number  
indicates the posterior probability that the function is concave down, with  
278 generalists having lower extinction risk/greater duration than either type of  
specialist. Note that the inflection point/optimum of Fig. 3 is approximately  
280  $x = 0$ , something that is expected given the estimate of  $\mu_v$  (Fig. 2).

The matrix  $\Sigma$  describing the covariance between the different coefficients

describes how these coefficients might vary together across the origination cohorts. Similar to how this was modeled (Eq. 1, 2), for interpretation purposes  $\Sigma$  can be decomposed into a vector of standard deviations  $\vec{\tau}$  and a correlation matrix  $\Omega$ .

The estimates of the standard deviation of between-cohort coefficient estimates  $\tau$  indicate that some effects can vary greatly between-cohorts (Fig. 4). Coefficients with greater values of  $\tau$  have greater between-cohort variation. The covariate effects with the greatest between origination cohort variation are  $\beta_r$ ,  $\beta_v$ , and  $\beta_{v^2}$ . Estimates of  $\beta_m$  have negligible between cohort variation, as there is less between cohort variation than the between cohort variation in baseline extinction risk  $\beta_0$ . However the amount of between cohort variation in estimates of  $\beta_{v^2}$  means that it is possible for the function describing the effect of environmental affinity to be upward facing for some cohorts (Eq. 3), which corresponds to environmental generalists being shorted lived than specialists in that cohort.

The correlation terms of  $\Omega$  (Fig. 5) describe the relationship between the coefficients and how their estimates may vary together across cohorts. The correlations between the intercept term  $\beta_0$  and the effects of the taxon traits are of particular interest for evaluating the Jablonski (1986) scenario (Fig. 5 first column/last row). Keep in mind that when  $\beta_0$  is low, extinction risk is low; and conversely, when  $\beta_0$  is high, then extinction risk is high.

Marginal posterior probabilities of the correlations between the level of baseline extinction risk  $\beta_0$  and the effects of the taxon traits indicate that the correlation between expected extinction risk and both geographic range  $\beta_r$  and  $\beta_{v^2}$  are of particular note (Fig. 6).

There is approximately a 98% probability that  $\beta_0$  and  $\beta_r$  are negatively

308 correlated (Fig. 6), meaning that as extinction risk increases, the  
effect/importance of geographic range on genus duration increases. This means  
310 that increases in baseline extinction rate are correlated with an increased  
importance of geographic range size. There is a 94% probability that  $\beta_0$  and  $\beta_{v^2}$   
312 are negatively correlated (Fig. 6), meaning that as extinction risk increases, the  
peakedness of  $f(v_i)$  increases and the relationship tends towards concave down.  
314 Additionally, there is a 97% probability that values of  $\beta_r$  and  $\beta_{v^2}$  are positively  
correlated (Mean correlation 0.51, standard deviation 0.23).

316 While the overall group level estimates are of particular importance when  
defining time-invariant differences in extinction risk, it is also important and  
318 useful to analyze the individual level parameter estimates in order to better  
understand how parameters actually vary across cohorts.

320 In comparison to the overall mean extinction risk  $\mu_0$ , cohort level estimates  $\beta_0$   
show some amount of variation through time as expected by estimates of  $\tau_0$   
322 (Fig. 7). A similar, if slightly greater, amount of variation is also observable in  
cohort estimates of the effect of geographic range  $\beta_r$  (Fig. 8). Again, smaller  
324 values of  $\beta_0$  correspond to lower expected extinction risk. Similarly, smaller  
values of  $\beta_r$  correspond to greater decrease in extinction risk with increasing  
326 geographic range

How the effect of environmental affinity varies between cohorts can be observed  
328 by using the cohort specific coefficients estimates. Following the same procedure  
used earlier (Fig. 4), but substituting cohort specific estimates of  $\beta_v$  and  $\beta_{v^2}$  for  
330  $\mu_v$  and  $\mu_{v^2}$ , the cohort specific effect of environmental preference as a multiplier  
of mean extinction risk can be calculated. This was done only for the Weibull  
332 model, though the observed pattern should be similar for the exponential model.

As expected based on the estimates of  $\tau_v$  and  $\tau_{v^2}$ , there is greater variation in

334 the peakedness of  $f(v_i)$  than there is variation between concave up and down  
 functions (Fig. 9). 9 of the 33 cohorts have less than 50% posterior probability  
 336 that generalists are potentially expected to be shorter lived than specialists,  
 though two of those cases have approximately a 50% probability of being either  
 338 concave up or down. This is congruent with the 0.86 posterior probability that  
 $\mu_{v^2}$  is positive/ $f(v_i)$  is concave down.  
 340 Additionally, for some cohorts there is a quite striking pattern where the effect  
 of environmental preference  $v$  has a nearly-linear relationship (Fig. 9). These are  
 342 primarily scenarios where one of the end member preferences is expected to  
 have a greater duration than either intermediate or the opposite end member  
 344 preference. Whatever curvature is present in these nearly-linear cases is due to  
 the definition of  $f(v)$  as it is not defined for non-negative values of  $\sigma$  (Eq. 3). For  
 346 most of the all stages between the Emsian through the Tournaisian, inclusive,  
 intermediate preferences are of intermediate extinction risk when compared with  
 348 epicontinental specialists (lowest risk) or open-ocean specialists (highest risk).  
 This time period represents most of the Devonian.

## 350 4 Discussion

My results demonstrate that both the effects of geographic range and the  
 352 peakedness/concavity of environmental preference are both negatively  
 correlated with baseline extinction risk, meaning that as baseline extinction risk  
 354 increases the effect sizes of both these traits are expected to increase (Fig. 6).  
 This result supports neither of the two proposed macroevolutionary mechanisms  
 356 for how biological traits should correlate with extinction risk. The observed  
 correlation between the two effects as well as between the effects and baseline  
 358 extinction risk instead implies that as baseline extinction risk increases, the



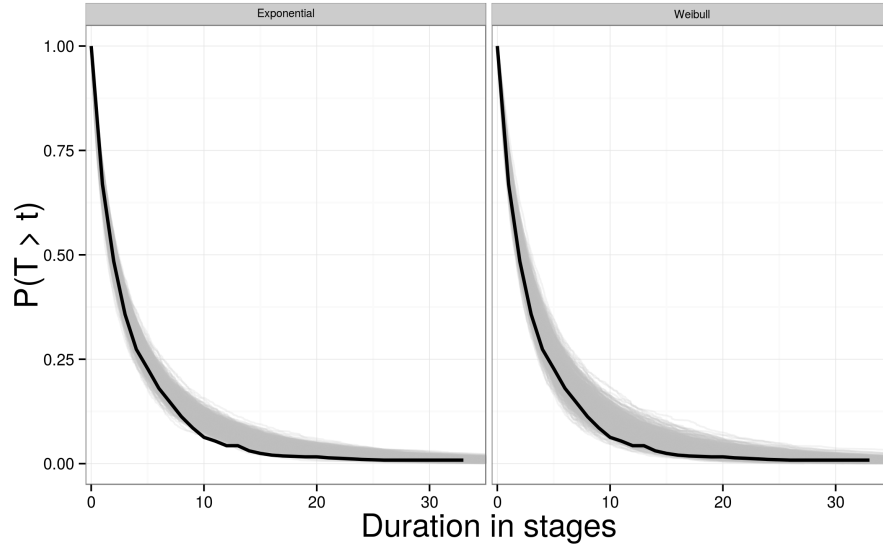


Figure 1: Comparison of empirical estimates of  $S(t)$  versus estimates from 1000 posterior predictive data sets.  $S(t)$  corresponds to  $P(T > t)$  as it is the probability that a given genus observed at age  $t$  will continue to live. This is equivalent to the probability that  $t$  is less than the genus' ultimate duration  $T$ . Note that the Weibull (left) model has noticeably better fit to the data than the exponential (right).

strength of the total selection gradient on biological traits (except body size)  
 360 increases. This manifests as greater differences in extinction risk for each unit  
 difference in the biological covariates during periods of high extinction risk,  
 362 while a relatively flatter selection gradient during periods of low extinction risk.

There are two mass extinction events that are captured within the time frame  
 364 considered here: the Ordovician-Silurian and the Frasnian-Famennian. The  
 cohorts bracketing these events are worth considering in more detail.

366 The proposed mechanism for the end Ordovician mass extinction is a decrease  
 in sea level and the draining of epicontinental seas due to protracted glaciation  
 368 (Johnson, 1974, Sheehan, 2001). My results are broadly consistent with this  
 scenario with both epicontinental and open-ocean specialists having a much

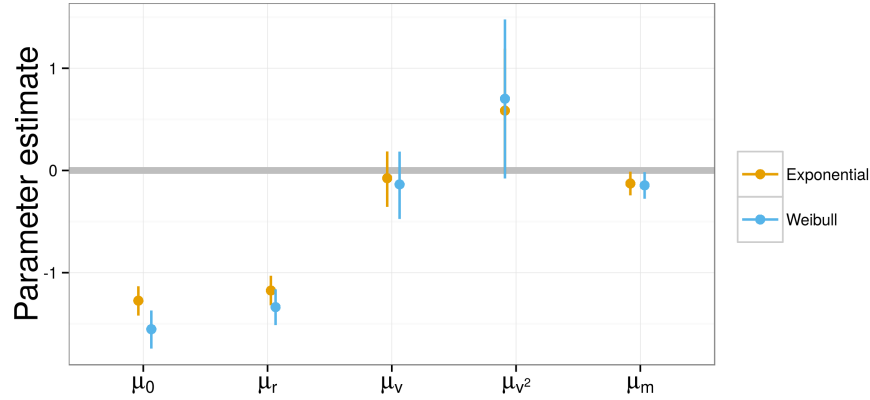


Figure 2: Estimates of the overall effects of the covariates on extinction risk. Included is also the estimate of  $\mu_0$  which corresponds to the intercept term or, because of standardization, the overall mean expected extinction risk. Estimates are presented for both the exponential (gold) and Weibull (blue) models. The point corresponds to the median of the posterior distribution, while the error bars correspond to the 80% credible intervals of the estimates.

370 lower expected duration than intermediate taxa (Fig. 9). All of the stages  
between the Darriwillian and the Llandovery, except the Hirnantian, have a  
372 greater than expected probability that  $f(v)$  is concave down. The pattern for  
the Darriwillian, which marks the supposed start of Ordovician glacial activity,  
374 demonstrates that taxa tend to favor open-ocean environments are expected to  
have a greater duration than either intermediate or epicontinental specialists, in  
376 decreasing order.

For nearly the entire Devonian estimates of  $f(v)$  indicate that one of the  
378 environmental end members is favored over the other end member of  
intermediate preference (Fig. 9). This is consistent with Miller and Foote (2009).  
380 For the Givetian though the end of the Devonian and into the Tournaisian, I  
find that epicontinental favoring taxa are expected to have a greater duration  
382 than either intermediate or open-ocean specialists. Additionally, for nearly the

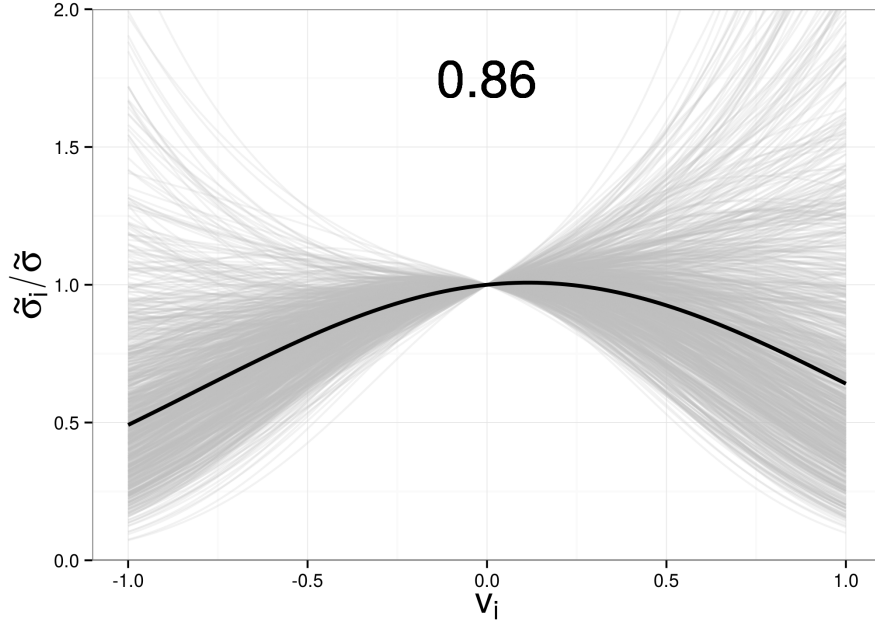


Figure 3: The overall expected relationship  $f(v_i)$  between environmental affinity  $v_i$  and a multiplier of extinction risk (Eq. 3). Each grey line corresponds to a single draw from the posterior predictive distribution, while the black corresponds to the median of the posterior predictive distribution. The overall shape of  $f(v_i)$  is concave down with an optimum of close 0, which corresponds to affinity approximately equal to the expectation based on background environmental occurrence rates.

entire Devonian except the Eifelian and through the Viséan, the cohort-specific  
estimates of  $f(v)$  are concave-up. This is the opposite pattern than what is  
expected (Fig. 3). This result, however, seems to reflect the intensity of the  
seemingly nearly-linear difference in expected duration across the range of  $v$ ) as  
opposed to an inversion of the weakly expected curvilinear pattern.

There is an approximate 86% posterior probability that taxa with intermediate  
environmental preferences are possibly expected to have a lesser extinction risk  
than either end members, the over all curvature of  $f(v_i)$  is not very peaked,  
meaning that this relationship does not lead to very strong differences in

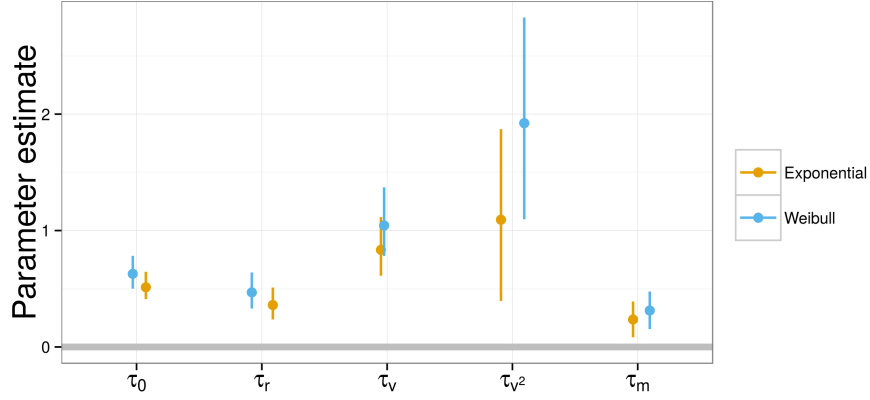


Figure 4: Estimates of the scale parameters describing the expected differences in the effect of the covariates, and of the intercept/baseline extinction risk, between cohorts. Higher values of  $\tau$  correspond to greater expected differences between cohorts. Estimates are presented for both the exponential (gold) and Weibull (blue) models. The point corresponds to the median of the posterior distribution, while the error bars correspond to the 80% credible intervals of the estimates.

392 extinction risk (Fig. 3). This result gives weak support for the hypothesis that,  
in general, environmental generalists survive for longer than environmental  
394 specialists (Liow, 2004, 2007, Nürnberg and Aberhan, 2013, 2015, Simpson,  
1944).

396 The variance in estimate of the overall  $f(v_i)$  reflects the large between cohort  
variance in cohort specific estimates of  $f(v_i)$  (Fig. 9). Given that there is only a  
398 86% posterior probability that the expected overall estimate of  $f(v_i)$  is concave  
down, it is not surprising that there are some stages where the theorized  
400 relationship is in fact reversed. Additionally, as discussed earlier, some of those  
same stages where  $f(v_i)$  does not resemble the theorized nonlinear relation with  
402 the optimum in the middle, but are instead is highly skewed or effectively linear  
(Fig. 9).

404 These results do not necessarily refute “survival of the unspecialized” as a

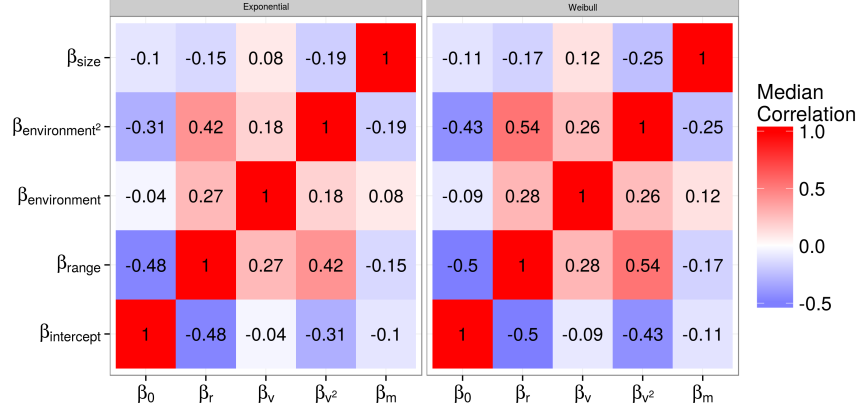


Figure 5: Heatmap for the median estimates of the terms of the correlation matrix  $\Omega$  between cohort-level covariate effects. Both the exponential (left) and Weibull (right) models are presented. The off-diagonal terms are the correlation between the estimates of the cohort-level estimates of the effects of covariates, along with intercept/baseline extinction risk.

time-invariant generalization, but instead demonstrate how, while the expected group-level estimate of  $f(v_i)$  might favor one hypothesis, there is still enough variability between cohorts so that in some realizations this pattern may not hold or can even be reversed. These results are also consistent with aspects of Miller and Foote (2009) who found that the effect of environmental preference on extinction risk was quite variable and without obvious patterning during times of background extinction.

This model can be improved through either increasing the number of analyzed taxon traits, expanding the hierarchical structure of the model to include other major taxonomic groups of interest, and the inclusion of explicit phylogenetic relationships between the taxa in the model as an additional hierarchical effect.

An example taxon trait that may be of particular interest is the affixing strategy or method of interaction with the substrate of the taxon. This trait has been found to be related to brachiopod survival (Alexander, 1977) so its

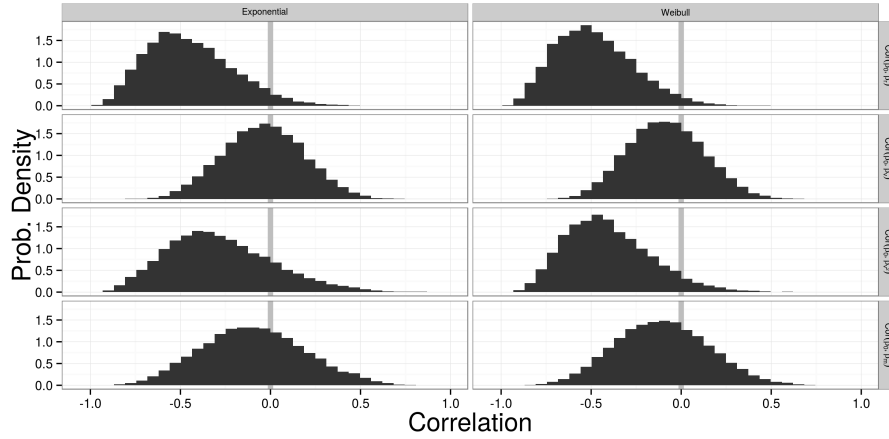


Figure 6: Marginal posterior distributions of the correlations between intercept terms/baseline extinction risk and the effects of each of the covariates. These are presented for both the exponential (left) and Weibull (right) models.

inclusion may be of particular interest.

420 It is theoretically possible to expand this model to allow for comparisons within  
and between major taxonomic groups. This approach would better constrain the  
422 brachiopod estimates while also allowing for estimation of similarities and  
differences in cross-taxonomic patterns. The major issue surrounding this  
424 particular expansion involves finding an similarly well sampled taxonomic group  
that is present during the Paleozoic. Example groups include Crinoidea,  
426 Ostracoda, and other “Paleozoic” groups (Sepkoski Jr., 1981).

Taxon traits like environmental preference or geographic range (Hunt et al.,  
428 2005, Jablonski, 1987) are most likely heritable, at least phylogenetically  
(Housworth et al., 2004, Lynch, 1991). Without phylogenetic context, this  
430 analysis assumes that differences in extinction risk between taxa are  
independent of those taxa’s shared evolutionary history (Felsenstein, 1985). In  
432 contrast, the origination cohorts only capture shared temporal context. The  
inclusion of phylogenetic context as an addition individual level hierarchical

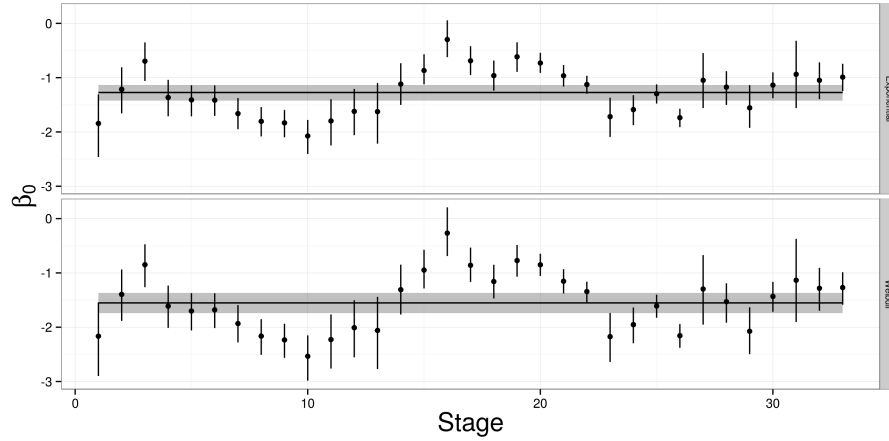


Figure 7: Comparison of cohort-specific estimates of  $\beta_0$  presented along with the estimate for the overall baseline extinction risk. Points correspond to the median of the cohort-specific estimate, along with 80% credible intervals. The horizontal line is the median estimate of the overall baseline extinction risk along with 80% credible intervals. Results are presented for the exponential (top) and Weibull (bottom) models.

434 structure independent of origination cohort would allow for determining how  
much of the observed variability is due to shared evolutionary history versus  
436 actual differences associated with these taxonomic traits. For example, it has  
been shown that phylogeny contribute non-trivially to differences in mammal  
438 species durations SMITS IN PREP.

In summary, patterns of Paleozoic brachiopod survival were analyzed using a  
440 fully Bayesian hierarchical survival modelling approach. Using a varying-slopes,  
varying-intercepts approach I am able to model both the overall mean effect of  
442 biological covariates on extinction risk while also modeling the correlation  
between origination cohort-specific estimates of covariate effects. I find that as  
444 baseline extinction risk increases, the strength of the selection gradient on  
biological traits (except body size) increases. This manifests as greater  
446 differences in extinction risk for each unit difference in the biological covariates

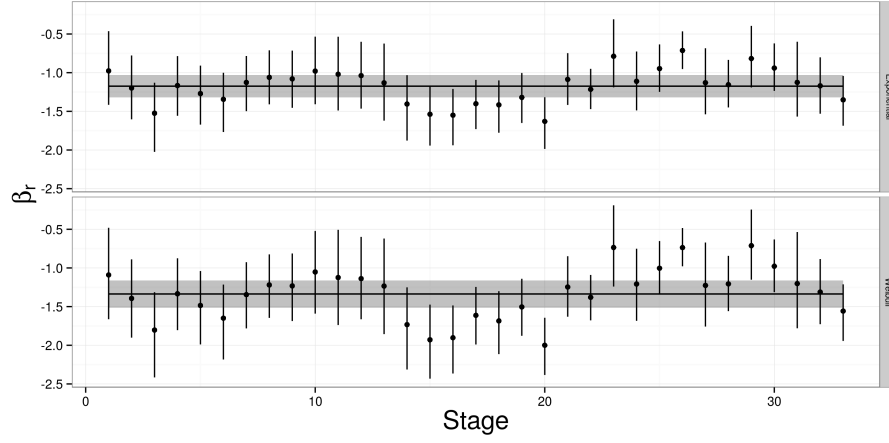


Figure 8: Comparison of cohort-specific estimates of the effect of geographic range on extinction risk  $\beta_r$ , presented along with the estimate for the overall effect of geographic range. Points correspond to the median of the cohort-specific estimate, along with 80% credible intervals. The horizontal line is the median estimate of the overall baseline extinction risk along with 80% credible intervals. Results are presented for the exponential (top) and Weibull (bottom) models.

during periods of high extinction risk, while a much flatter total selection  
 448 gradient during periods of low extinction risk. I also find some support for  
 “survival of the unspecialized” (Liow, 2004, 2007, Nürnberg and Aberhan, 2013,  
 450 2015, Simpson, 1944) as a general characterization of the effect of environmental  
 preference on extinction risk (Fig. 3), though there is heterogeneity between  
 452 origination cohorts (Fig. 9). Generally, this study demonstrates the advantages  
 of a hierarchical Bayesian framework for taking into account the structured  
 454 nature of the data. Future studies of structured data should adopt similar  
 strategies in order to best model our knowledge instead of ignoring that  
 456 structure which can lead to poor and/or incorrect inference.



## Acknowledgements

458 I would like to thank K. Angielczyk, M. Foote, P. D. Polly, and R. Ree for  
helpful discussion and advice. Additionally, thank you A. Miller for the  
460 epicontinental versus open-ocean assignments. This entire study would would  
not have been possible without the Herculean effort of the many contributors to  
462 the Paleobiology Database. In particular, I would like to thank NAMES. This is  
Paleobiology Database publication XXX.

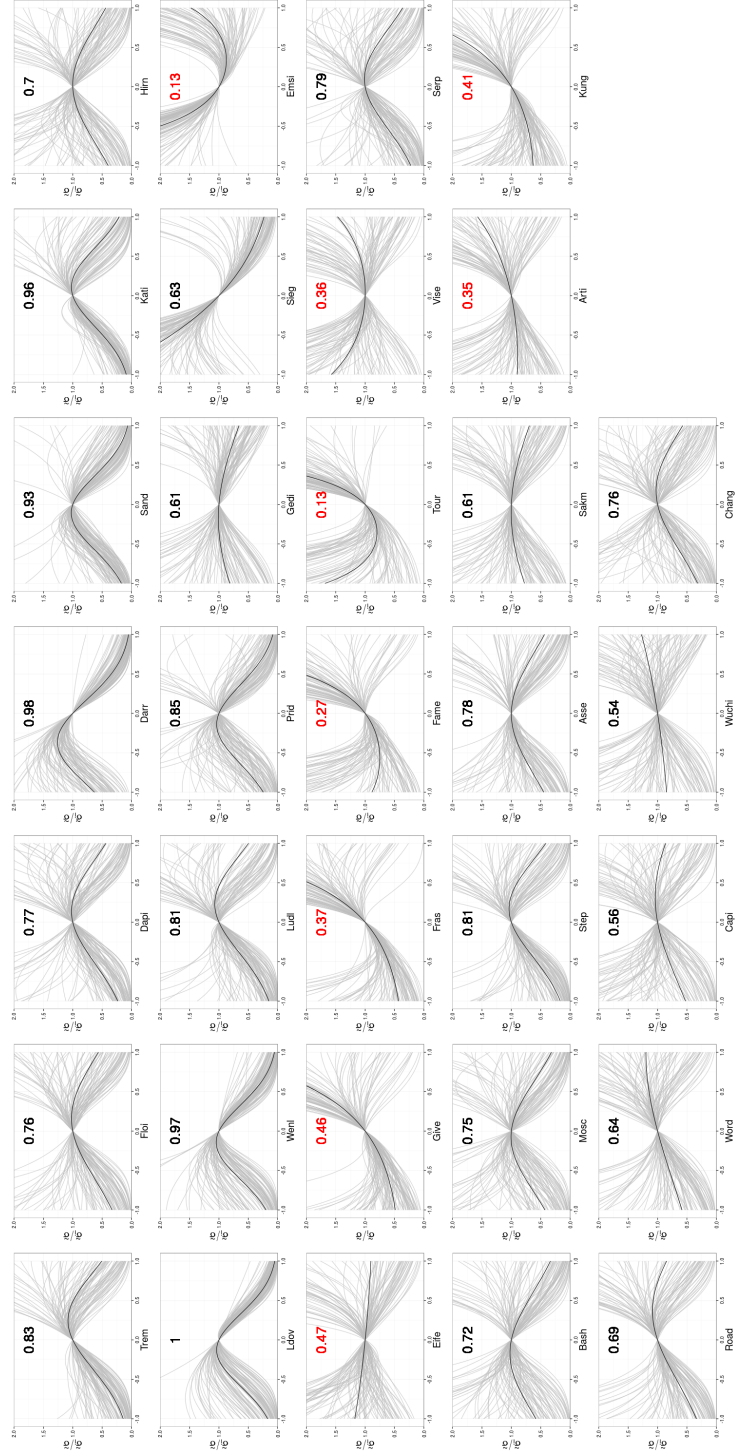


Figure 9: Comparison of the cohort-specific estimates of  $f(v_i)$  (Eq. 3) for the 33 analyzed origination cohorts. The stage of origination is labeled on the x-axis of each panel. The oldest stage is in the upper left, while the youngest is in the lower left. The number in each panel corresponds to the posterior probability that  $f(v_i)$  is concave down. Those that are highlighted in red have less than 51% posterior predictive probability that  $f(v_i)$  is concave down.

## References

- Alexander, R. R., 1977. Generic longevity of articulate brachiopods in relation  
to the mode of stabilization on the substrate. *Palaeogeography,*  
*Palaeoclimatology, Palaeoecology* 21:209–226.
- Baumiller, T. K., 1993. Survivorship analysis of Paleozoic Crinoidea: effect of  
filter morphology on evolutionary rates. *Paleobiology* 19:304–321.
- Cooper, W. S., 1984. Expected time to extinction and the concept of  
fundamental fitness. *Journal of Theoretical Biology* 107:603–629.
- Felsenstein, J., 1985. Phylogenies and the comparative method. *American*  
*Naturalist* 125:1–15. URL <http://www.jstor.org/stable/2461605>.
- Foote, M., 1988. Survivorship analysis of Cambrian and Ordovician Trilobites.  
*Paleobiology* 14:258–271.
- , 2006. Substrate affinity and diversity dynamics of Paleozoic marine  
animals. *Paleobiology* 32:345–366. URL  
<http://www.bioone.org/doi/abs/10.1666/05062.1>.
- Foote, M. and A. I. Miller, 2013. Determinants of early survival in marine  
animal genera. *Paleobiology* 39:171–192. URL  
<http://www.bioone.org/doi/abs/10.1666/12028>.
- Gelman, A., 2006. Prior distributions for variance parameters in hierarchical  
models. *Bayesian Analysis* 1:515–533.
- Gelman, A., J. B. Carlin, H. S. Stern, D. B. Dunson, A. Vehtari, and D. B.  
Rubin, 2013. *Bayesian data analysis*. 3 ed. Chapman and Hall, Boca Raton,  
FL.

- Gelman, A. and J. Hill, 2007. Data Analysis using Regression and  
 488 Multilevel/Hierarchical Models. Cambridge University Press, New York, NY.
- Hijmans, R. J., 2015. raster: Geographic data analysis and modeling. URL  
 490 <http://CRAN.R-project.org/package=raster>. R package version 2.3-24.
- Hoffman, M. D. and A. Gelman, 2014. The No-U-Turn Sampler: Adaptively  
 492 Setting Path Lengths in Hamiltonian Monte Carlo. Journal of Machine  
 Learning Research 15:1351–1381.
- Housworth, E. A., P. Martins, and M. Lynch, 2004. The Phylogenetic Mixed  
 494 Model. The American Naturalist 163:84–96.
- Hunt, G., K. Roy, and D. Jablonski, 2005. Species-level heritability reaffirmed: a  
 496 comment on "On the heritability of geographic range sizes". American  
 498 Naturalist 166:129–135.
- Ibrahim, J. G., M.-H. Chen, and D. Sinha, 2001. Bayesian Survival Analysis.  
 500 Springer, New York.
- Jablonski, D., 1986. Background and mass extinctions: the alternation of  
 502 macroevolutionary regimes. Science 231:129–133.
- , 1987. Heritability at the species level: analysis of geographic ranges of  
 504 cretaceous mollusks. Science 238:360–363. URL  
<http://www.ncbi.nlm.nih.gov/pubmed/17837117>.
- Jablonski, D. and K. Roy, 2003. Geographical range and speciation in fossil and  
 506 living  
 molluscs. Proceedings. Biological sciences / The Royal Society 270:401–6. URL  
 508 <http://www.pubmedcentral.nih.gov/articlerender.fcgi?artid=1691247&tool=pmcentrez&rendertype>
- Johnson, J. G., 1974. Extinction of Perched Faunas. Geology 2:479–482.  
 510

- Kiessling, W. and M. Aberhan, 2007. Environmental determinants of marine  
512 benthic biodiversity dynamics through Triassic–Jurassic time. *Paleobiology*  
33:414–434.
- 514 Klein, J. P. and M. L. Moeschberger, 2003. *Survival Analysis: Techniques for*  
Censored and Truncated Data. 2nd ed. Springer, New York.
- 516 Liow, L. H., 2004. A test of Simpson’s “rule of the survival of the relatively  
unspecialized” using fossil crinoids. *The American naturalist* 164:431–43.  
518 URL <http://www.ncbi.nlm.nih.gov/pubmed/15459876>.
- , 2007. Does versatility as measured by geographic range, bathymetric  
520 range and morphological variability contribute to taxon longevity? *Global*  
*Ecology and Biogeography* 16:117–128. URL  
522 <http://doi.wiley.com/10.1111/j.1466-8238.2006.00269.x>  
[papers2://publication/doi/10.1111/j.1466-8238.2006.00269.x](http://publication/doi/10.1111/j.1466-8238.2006.00269.x).
- 524 Lynch, M., 1991. Methods for the analysis of comparative data in evolutionary  
biology. *Evolution* 45:1065–1080.
- 526 Miller, A. I. and S. R. Connolly, 2001. Substrate affinities of higher taxa and  
the Ordovician Radiation. *Paleobiology* 27:768–778. URL  
528 <http://www.bioone.org/doi/abs/10.1666/0094-8373%282001%29027%3C0768%3ASAOHTA%3E2.O.CO%3B2>.
- Miller, A. I. and M. Foote, 2009. Epicontinental seas versus open-ocean settings:  
530 the kinetics of mass extinction and origination. *Science* 326:1106–9. URL  
<http://www.ncbi.nlm.nih.gov/pubmed/19965428>.
- 532 Nürnberg, S. and M. Aberhan, 2013. Habitat breadth and geographic range  
predict diversity dynamics in marine Mesozoic bivalves. *Paleobiology*  
534 39:360–372. URL <http://www.bioone.org/doi/abs/10.1666/12047>.
- , 2015. Interdependence of specialization and biodiversity in Phanerozoic

536 marine invertebrates. *Nature communications* 6:6602. URL  
<http://www.ncbi.nlm.nih.gov/pubmed/25779979>.

538 Palmer, M. E. and M. W. Feldman, 2012. Survivability is more fundamental  
than evolvability. *PloS one* 7:e38025. URL  
540 <http://www.pubmedcentral.nih.gov/articlerender.fcgi?artid=3377627&tool=pmcentrez&rendertype>

Payne, J. L. and S. Finnegan, 2007. The effect of geographic range on  
542 extinction risk during background and mass extinction. *Proceedings of the  
National Academy of Sciences* 104:10506–11. URL  
544 <http://www.pubmedcentral.nih.gov/articlerender.fcgi?artid=1890565&tool=pmcentrez&rendertype>

Payne, J. L., N. A. Heim, M. L. Knope, and C. R. McClain, 2014. Metabolic  
546 dominance of bivalves predates brachiopod diversity decline by more than 150  
million years. *Proceedings of the Royal Society B* 281:20133122.

548 Raup, D. M., 1975. Taxonomic survivorship curves and Van Valen’s Law.  
*Paleobiology* 1:82–96. URL  
550 <http://www.ncbi.nlm.nih.gov/pubmed/17777225>.

———, 1978. Cohort Analysis of generic survivorship. *Paleobiology* 4:1–15.

552 Sepkoski Jr., J. J., 1981. A factor analytic description of the Phanerozoic  
marine fossil record. *Paleobiology* 7:36–53.

554 Sheehan, P., 2001. The late Ordovician mass extinction. *Annual Review of  
Earth and Planetary Sciences* 29:331–364. URL  
556 <http://www.annualreviews.org/doi/abs/10.1146/annurev.earth.29.1.331>.

Simpson, C., 2006. Levels of selection and large-scale morphological trends.  
558 Ph.D. thesis, University of Chicago.

Simpson, C. and P. G. Harnik, 2009. Assessing the role of abundance in marine

- 560 bivalve extinction over the post-Paleozoic. *Paleobiology* 35:631–647. URL  
<http://www.bioone.org/doi/abs/10.1666/0094-8373-35.4.631>.
- 562 Simpson, G. G., 1944. *Tempo and Mode in Evolution*. Columbia University  
 Press, New York.
- 564 ———, 1953. *The Major Features of Evolution*. Columbia University Press,  
 New York.
- 566 Stan Development Team, 2014a. Stan: A c++ library for probability and  
 sampling, version 2.5.0. URL <http://mc-stan.org/>.
- 568 ———, 2014b. *Stan Modeling Language Users Guide and Reference Manual*,  
 Version 2.5.0. URL <http://mc-stan.org/>.
- 570 Van Valen, L., 1973. A new evolutionary law. *Evolutionary Theory* 1:1–30.  
 URL <http://ci.nii.ac.jp/naid/10011264287/>.
- 572 ———, 1979. Taxonomic survivorship curves. *Evolutionary Theory* 4:129–142.
- Wang, S. C., 2003. On the continuity of background and mass extinction.  
 574 *Paleobiology* 29:455–467. URL  
<http://www.bioone.org/doi/abs/10.1666/0094-8373%282003%29029%3C0455%3AOTCOBA%3E2.0.CO%3B2>.
- 576 Watanabe, S., 2010. Asymptotic Equivalence of Bayes Cross Validation and  
 Widely Applicable Information Criterion in Singular Learning Theory.  
 578 *Journal of Machine Learning Research* 11:3571–3594.

## A Uncertainty in environmental preference

580 The calculation and inclusion of environmental affinity in the survival model is a  
statistical procedure that takes into account our uncertainty based on where  
582 fossils tend to occur. Because we cannot directly observe if a fossil taxon had  
occurrences restricted to only a single environment, instead we can only  
584 estimate its affinity with uncertainty. One advantage of using a Bayesian  
analytical approach is that both parameters and data are considered random  
586 samples from some underlying distribution, which means that it is possible to  
model the uncertainty in our covariates of interest (Gelman et al., 2013). My  
588 approach is conceptually similar to Simpson and Harnik (2009) but instead of  
obtaining a single point estimate, an entire posterior distribution is estimated.

590 The first step is to determine the probability  $\theta$  at which genus  $i$  occurs in an  
epicontinental settings based on its own pattern of occurrences. Define  $e_i$  as the  
592 number of occurrences of genus  $i$  in an epicontinental sea and  $o_i$  as the number of  
occurrences of genus  $i$  not in an epicontinental sea (e.g. open ocean). Because  
594 the value of interest is the probability of occurring in an epicontinental  
environment, given the observed fossil record, I assume that probability follows  
596 a binomial distribution. We can then define our sampling statement as

$$e_i \sim \text{Binomial}(e_i + o_i, \theta_i). \quad (4)$$

I used a flat prior for  $\theta_i$  defined as  $\theta_i \sim \text{Beta}(1, 1)$ . Because the beta  
598 distribution is the conjugate prior for the binomial distribution, the posterior is  
easy to compute in closed form. The posterior probability of  $\theta$  is then

$$\theta_i \sim \text{Beta}(e_i + 1, o_i + 1) \quad (5)$$



600 It is extremely important, however, to take into account the overall  
 environmental occurrence probability of all other genera present at the same  
 602 time as genus  $i$ . This is incorporated as an additional probability  $\Theta$ . Define  $E_i$   
 as the total number of other fossil occurrences (except for genus  $i$ ) in  
 604 epicontinental seas during stages where  $i$  occurs and  $O_i$  as the number of other  
 fossil occurrences not on epicontinental seas. We can then define the sampling  
 606 statement as

$$E_i \sim \text{Binomial}(E_i + O_i, \Theta_i). \quad (6)$$

Again, I used a flat prior of  $\Theta_i$  defined as  $\Theta_i \sim \text{Beta}(1, 1)$ . The posterior of  $\Theta$  is  
 608 then simply defined as

$$\Theta_i \sim \text{Beta}(E_i + 1, O_i + 1) \quad (7)$$

I then define the environmental affinity of genus  $i$  as  $v_i = \theta_i - \Theta_i$ .  $v_i$  is a value  
 610 that can range between -1 and 1, where negative values indicate that genus  $i$   
 tends to occur more frequently in open ocean environments than background  
 612 while positive values indicate that genus  $i$  tends to occur in epicontinental  
 environments.

614 While this approach is noticeably more complicated than previous ones (Foote,  
 2006, Kiessling and Aberhan, 2007, Miller and Connolly, 2001, Simpson and  
 616 Harnik, 2009) there are some important benefits to both using a continuous  
 measure of affinity as well directly modeling our uncertainty. In order to show  
 618 some of these benefits, I performed a simulation analysis of how  
 modal/maximum *a posteriori* (MAP) estimates versus full posterior estimates.

620 In this simulation, I first defined the “background” epicontinental occurrence  $\theta_b$   
 as 0.50 with a small amount of noise. This was represented as a beta distribution

$$\Theta_b = \text{Beta}(\alpha = 2500, \beta = 2500). \quad (8)$$

622 This choice of parameters for the distribution reflects the average number of  
background occurrences for either epicontinental or open ocean environments  
624 per genus.

Using this background occurrence ratio, I randomly generated the occurrence  
626 patterns of 1000 simulated taxa. This was done at multiple sample sizes (1, 2, 3,  
4, 5, 10, 25, 50, 100) in order to demonstrate the effects of increasing sample  
628 size on the confidence of environmental affinity. For each simulated taxon I  
calculated the full posterior distribution while assuming a flat Beta prior  
630 (Beta(1, 1)). Using the full posterior I calculated the MAP probability of  
occurring in epicontinental environments. The environmental affinity was  
632 calculated for each of the simulated taxa using both the full posterior and the  
MAP estimate. In this toy example, environmental affinity can range between  
634 -0.5 and 0.5.

As should be expected, as sample size increases the distribution of MAP  
636 estimates converge on the true value (Fig. 10). For taxa with less than 10  
occurrences, the MAP estimate is biased towards extreme values. Note that the  
638 mode of the beta distribution is not defined for situations where there were 0  
draws of one of the environmental conditions. Instead, the vertical line is based  
640 entirely on the observed occurrences which are technically the modal estimates  
because they are the most frequently occurring/highest density.

642 In contrast, we can compare the true occurrence probability distribution versus  
the posterior estimate for a given sample (Fig. 11). When sample sizes are low,  
644 posterior estimates are flat and represent a compromise between the likelihood  
and the flat prior (Eq. 5). Because of this, estimates from small sizes are less

likely to be overly biased towards the extremes. This is further emphasized by inspection of the estimates of environmental affinity for the simulated taxa (Fig. 12). Posterior estimates from simulated taxa with small sample size have a much broader distribution that both allows for the extreme observation but still captures the “true” value (0).

By defining environmental preference as the difference in full posterior estimates of occurrence probability, it is possible to include taxa with low sample sizes that are normally discarded (Foote, 2006, Kiessling and Aberhan, 2007, Miller and Connolly, 2001, Simpson and Harnik, 2009). Additionally, 55+% of observed Paleozoic brachiopod genera have less than 10 occurrences which is the range of sample sizes where MAP (or ML) estimates would be potentially most biased. This is preferable to finding the difference between the MAP estimates (blue line; Fig. 12).

## B Survival model

The simplest model of genus duration includes no covariate or structural information. Define  $y_i$  as the duration in stages of genus  $i$ , where  $i = 1, \dots, n$  and  $n$  is the number of observed genera. These two models are then simply defined as

$$\begin{aligned} y_i &\sim \text{Exponential}(\lambda) \\ y_i &\sim \text{Weibull}(\alpha, \sigma). \end{aligned} \tag{9}$$

$\lambda, \alpha$ , and  $\sigma$  are all defined for all positive reals. Note that  $\lambda$  is a “rate” or inverse-scale while  $\sigma$  is a scale parameter, meaning that  $\frac{1}{\lambda} = \sigma$ .

These simple models can then be expanded to include covariate information as predictors by reparameterizing  $\lambda$  or  $\sigma$  as a regression (Klein and Moeschberger,

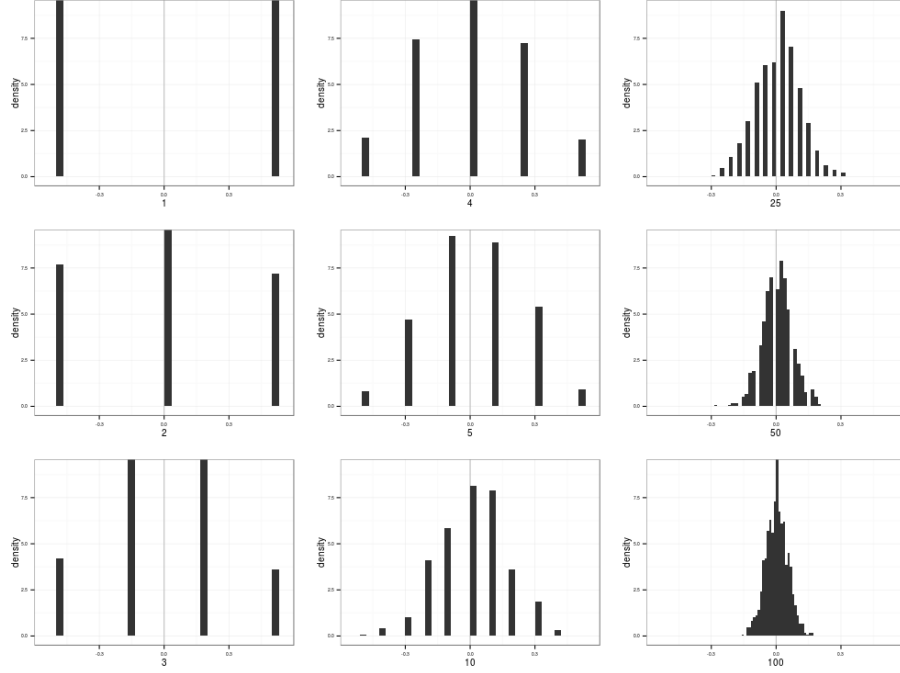


Figure 10: Histograms of the distributions of from the beta distribution defined in Eq. 8. As to be expected, as sample size increases the draws better resemble the underlying true distribution. Sample size is indicated as the label of the x-axis, increasing in column major order.

2003). Each of the covariates of interest is given its own regression coefficient (e.g.  $\beta_r$ ) along with an intercept term  $\beta_0$ . There are some additional complications to the parameterization of  $\sigma$  associated with the inclusion of  $\alpha$  as well as for interpretability (Klein and Moeschberger, 2003). Both of these are then written as

$$\begin{aligned}\lambda_i &= \exp(\beta_0 + \beta_r r_i + \beta_v v_i + \beta_{v^2} v_i^2 + \beta_m m_i) \\ \sigma_i &= \exp\left(\frac{-(\beta_0 + \beta_r r_i + \beta_v v_i + \beta_{v^2} v_i^2 + \beta_m m_i)}{\alpha}\right).\end{aligned}\tag{10}$$

The quadratic term for environmental affinity  $v$  is to allow for the possible nonlinear relationship between environmental affinity and extinction risk.

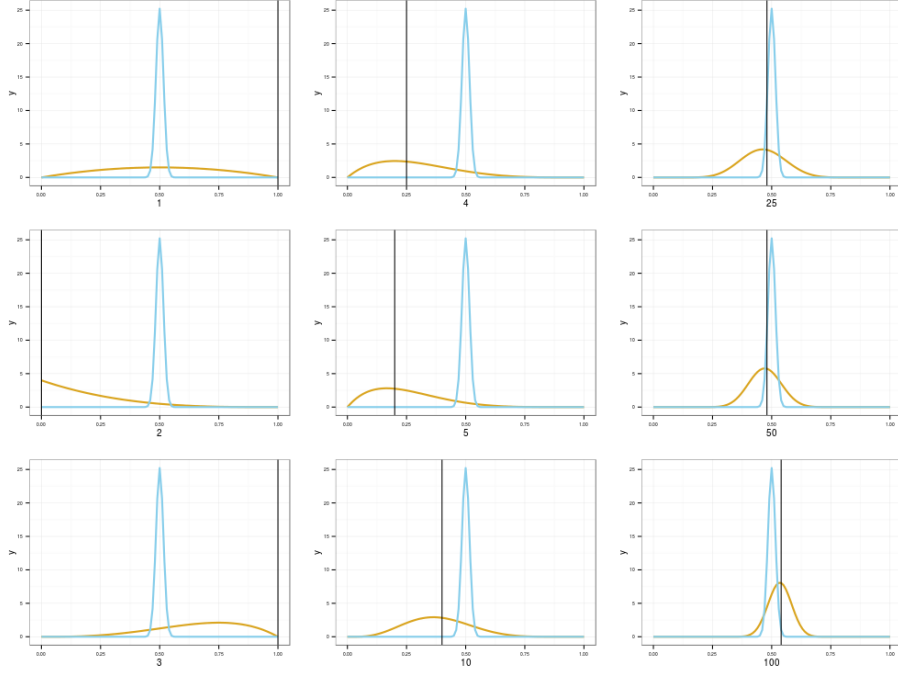


Figure 11: Comparisons of the underlying distribution (blue) to posterior estimates based on increasing sample size (gold). Each posterior estimate is represented for only a single realization of draws, each with sample size indicated as the x-axis label (increasing in column major order). Black vertical lines correspond to the MAP estimate of the simulated taxon’s affinity. This stands in contrast to the posterior distribution of expected affinity in gold.

The models which incorporate both equations 9 and 10 can then be further

676 expanded to allow all of the  $\beta$  coefficients, including  $\beta_0$ , to vary with origination  
cohort while also modeling their covariance and correlation. This is called a  
678 varying-intercepts, varying-slopes model (Gelman and Hill, 2007). It is much  
easier to represent and explain how this is parameterized using matrix notation.  
680 First, define  $\mathbf{B}$  as  $k \times J$  matrix of the  $k$  coefficients including the intercept term  
( $k = 5$ ) for each of the  $J$  cohorts. Second, define  $\mathbf{X}$  as a  $n \times k$  matrix where each  
682 column is one of the covariates of interest. Importantly,  $\mathbf{X}$  includes a columns of  
all 1s which correspond to the constant term  $\beta_0$ . Third, define  $j[i]$  as the

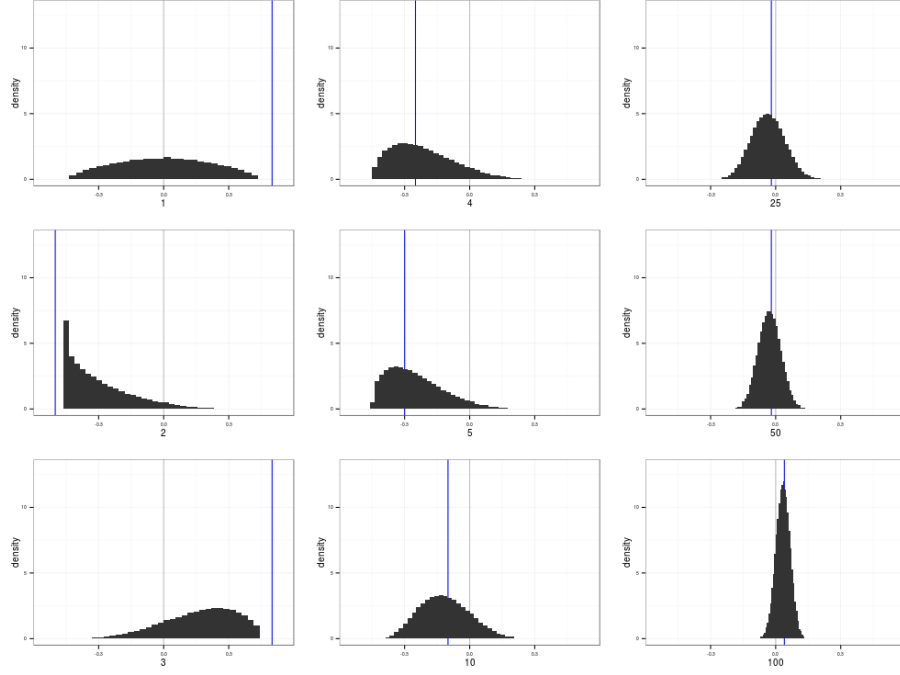


Figure 12: Histograms of the difference in the underlying occurrence distribution and the posterior distribution estimates from the previous graph (Fig. 11). The “true” value is included in all distributions of environmental affinities. Each affinity estimate is represented for only a single realization of draws, each with sample size indicated as the x-axis label (increasing in column major order). Blue vertical lines correspond to the difference in MAP estimates between the underlying distribution and the simulated taxon’s draws. This stands in contrast to the distribution of the differences between the simulated taxon and background.

684 origination cohort of genus  $i$ , where  $j = 1, \dots, J$  and  $J$  is the total number of  
observed cohorts. We then rewrite  $\lambda$  and  $\sigma$  of equation 10 in matrix notation as

$$\begin{aligned}\lambda_i &= \exp(\mathbf{X}_i B_{j[i]}) \\ \sigma_i &= \exp\left(\frac{-(\mathbf{X}_i B_{j[i]})}{\alpha}\right).\end{aligned}\tag{11}$$

686 Because  $B$  is a matrix, I use a multivariate normal prior with unknown vector

of means  $\mu$  and covariance matrix  $\Sigma$ . This is written as

$$B \sim \text{MVN}(\vec{\mu}, \Sigma) \quad (12)$$

688 where  $\vec{\mu}$  is length  $k$  vector representing the overall mean of the distributions of  
689  $\beta$  coefficients.  $\Sigma$  is a  $k \times k$  covariance matrix of the  $\beta$  coefficients.

690 What remains is assigning priors the elements of  $\vec{\mu}$  and the covariance matrix  $\Sigma$ .  
All elements of  $\vec{\mu}$  except for  $\mu_r$  were given weakly informative normal priors  
692 while  $\mu_r$  was given an informative normal prior ( $\mu_r \sim \mathcal{N}(-1, 1)$ ). The prior for  $\Sigma$   
is a bit more complicated due to its multivariate nature. Following the Stan  
694 Development Team (2014b), I modeled the scale terms separate from the  
correlation structure of the coefficients. This is possible because of the  
696 relationship between a covariance and a correlation matrix, defined as

$$\Sigma_B = \text{Diag}(\vec{\tau})\Omega\text{Diag}(\vec{\tau}) \quad (13)$$

where  $\vec{\tau}$  is a length  $k$  vector of variances and  $\text{Diag}(\tau)$  is a diagonal matrix.

698 I used a LKJ prior distribution for correlation matrix  $\Omega$  as recommended by  
Stan Development Team (2014b). The LKJ distribution is a single parameter  
700 multivariate distribution where values of the parameter  $\eta$  greater than 1  
concentrate density at the unit correlation matrix, which corresponds to no  
702 correlation between the  $\beta$  coefficients. The scale parameters,  $\vec{\tau}$ , are given weakly  
informative half-Cauchy ( $C^+$ ) priors following Gelman (2006).

## 704 C Censored observations

A key aspect of survival analysis is the inclusion of censored, or incompletely  
706 observed, data points (Ibrahim et al., 2001, Klein and Moeschberger, 2003). The  
two classes of censored observations encountered in this study were right and  
708 left censored observations. Right censored genera are those that did not go  
extinct during the window of observation, or genera that are still extant. Left  
710 censored observations are those taxa for which we know only an upper limit on  
their duration.

712 In the context of this study, I considered all genera that had a duration of only  
one geologic stage to be left censored as we do not have a finer degree of  
714 resolution.

The key function for modeling censored observations is the survival function, or  
716  $S(t)$ .  $S(t)$  corresponds to the probability that a genus having existed for  $t$  stages  
will not have gone extinct while  $h(t)$  corresponds to the instantaneous  
718 extinction rate at taxon age  $t$  Klein and Moeschberger (2003). For an  
exponential model,  $S(t)$  is defined as

$$S(t) = \exp(-\lambda t), \quad (14)$$

720 and for the Weibull distribution  $S(t)$  is defined as

$$S(t) = \exp\left(-\left(\frac{t}{\sigma}\right)^\alpha\right). \quad (15)$$

$S(t)$  is equivalent to the complementary cumulative distribution function,  
722  $1 - F(t)$  (Klein and Moeschberger, 2003).

For right censored observations, instead of calculating the likelihood as normal



724 (Eq. 11) the likelihood of an observation is evaluated using  $S(t)$ . Conceptually,  
this approach calculates the likelihood of observing a taxon that existed for at  
726 least that long. For left censored data, instead the likelihood is calculated using  
 $1 - S(t)$  which corresponds to the likelihood of observing a taxon that existed  
728 no longer than  $t$ .

The full likelihood statements incorporating fully observed, right censored, and  
730 left censored observations are then

$$\begin{aligned}\mathcal{L} &\propto \prod_{i \in C} \text{Exponential}(y_i | \lambda) \prod_{j \in R} S(y_j | \lambda) \prod_{k \in L} (1 - S(y_k | \lambda)) \\ \mathcal{L} &\propto \prod_{i \in C} \text{Weibull}(y_i | \alpha, \sigma) \prod_{j \in R} S(y_j | \alpha, \sigma) \prod_{k \in L} (1 - S(y_k | \alpha, \sigma))\end{aligned}\tag{16}$$

where  $C$  is the set of all fully observed taxa,  $R$  the set of all right censored taxa,  
732 and  $L$  the set of all left-censored taxa.

## D Widely applicable information criterion

734 WAIC can be considered a fully Bayesian alternative to the Akaike information  
criterion, where WAIC acts as an approximation of leave-one-out  
736 cross-validation which acts as a measure of out-of-sample predictive accuracy  
(Gelman et al., 2013). WAIC is calculated starting with the log pointwise  
738 posterior predictive density calculated as

$$\text{lppd} = \sum_{i=1}^n \log \left( \frac{1}{S} \sum_{s=1}^S p(y_i | \Theta^s) \right), \tag{17}$$

where  $n$  is sample size,  $S$  is the number posterior simulation draws, and  $\Theta$   
740 represents all of the estimated parameters of the model. This is similar to  
calculating the likelihood of each observation given the entire posterior. A

742 correction for the effective number of parameters is then added to lppd to  
adjust for overfitting. The effective number of parameters is calculated,  
744 following the recommendations of Gelman et al. (2013), as

$$p_{\text{WAIC}} = \sum_{i=1}^n V_{s=1}^S(\log p(y_i|\Theta^S)). \quad (18)$$

where  $V$  is the sample posterior variance of the log predictive density for each  
746 data point.

Given both equations 17 and 18, WAIC is then calculated

$$\text{WAIC} = \text{lppd} - p_{\text{WAIC}}. \quad (19)$$

748 When comparing two or more models, lower WAIC values indicate better  
out-of-sample predictive accuracy. Importantly, WAIC is just one way of  
750 comparing models. When combined with posterior predictive checks it is  
possible to get a more complete understanding of a model's fit to the data.